Organic Electronics 51 (2017) 54–61

Contents lists available at ScienceDirect

Organic Electronics

journal homepage: www.elsevier.com/locate/orgel

Flexible QLED and OPV based on transparent polyimide substrate with rigid alicyclic asymmetric isomer

Fu Li, Jiulin Shen, Xiangfu Liu, Zhonghuan Cao, Xiang Cai, Junli Li, Ke Ding, Jikang Liu, Guoli Tu*

Wuhan National Laboratory for Optoelectronics, Huazhong University of Science and Technology, Wuhan 430074, People's Republic of China

ARTICLE INFO

Article history:
Received 27 July 2017
Received in revised form
4 September 2017
Accepted 8 September 2017
Available online 8 September 2017

Keywords:
Polyimide
Rigid alicyclic
Imidization
Flexible substrate
QLED
OPV

ABSTRACT

A series of isomeric alicyclic-functionalized polyimide with chemical imidization and thermal imidization (CPI-x and TPI-x) were prepared from a rigid alicyclic-functionalized isomerism diamine, 5(6)-amino-1-(4-aminophenyl)-1,3,3-trimethylindane (DAPI). The influences of incorporation of the isomeric rigid alicyclic structure onto the backbone of the polymers were systematically investigated in terms of optical, thermal, mechanical, dielectric and surface properties, respectively. Due to the moderate chemical imidization condition, CPI-x series retain higher glass transition temperature (Tg) in the range of 329–429 °C than the Tg of TPI-x (from 321.9 °C to 370.7 °C). Therefore, the CPI-1 film based 5-DAPI was chosen as the flexible substrate. MoO_3 was chosen as the interface layer to improve the compatibility between PI substrate and the metal electrode. Then a ultra-thin layer of MoO_3 (3 nm)/Au(2 nm)/Ag(4 nm) was utilized to be the transparent electrode. After annealing at 220 °C for 0.5 h, zinc oxide (ZnO) was deposited onto the electrode to maintain the superior electron mobility and improve the transparency of the electrode. Consequently, the flexible quantum dots light emitting diode (QLED) obtained a high luminance of 5230 (cd/m^2) and EQE of 5.2%, meanwhile, a device performance of 4.36% was achieved in organic photovoltaic (OPV) devices.

1. Introduction

In the recent years, solution-processed quantum dots light emitting diode (QLED) and organic photovoltaic (OPV) have attracted attention with a promising future of being lightweight, flexible, and attainable via roll-to-roll manufacturing process with low cost [1–3]. Transparent polymer films were considered to be the preferred choice for transparent flexible substrate owning to their tremendous advantages such as light weight, good bending performance, rich species, and compatibilities with the roll-to-roll process that widely used in large-scale production [4–8]. In addition to excellent optical performances, thermal durability, low coefficient thermal expansion (CTE) and inertness to organic solvents were also required for transparent flexible substrates [2,9]. The candidates of transparent flexible substrate including poly(-ethylene terephthalate) (PET), polycarbonate (PC), poly-(ethylene-2,6-naphthalate) (PEN), polyester sulfone (PES), and transparent colorless polyimide (cPI). Among these substrate, due to cPI possessed outstanding chemical and irradiation resistance, high thermal stability, excellent optical and mechanical properties, transparent polyimides (PIs) are regarded a suitable candidates for flexible substrates [10–12]. In order to obtain transparent PI substrate, the structural modifications to PI have been comprehensively studied [13–16]. The efforts include incorporation of flexibilizing groups, asymmetric units, bulky substituents, alicyclic segments and fluorine-containing structures [14,17–24], which break the conjugation and decrease the formation of charge transfer complex (CTC) and chain packing. Then the transmittance, processability and solubility in organic solvents could be improved [13,14,19,25–27]. However, most of the transparent PI based on 2,2′-bis(3,4-dicarboxyphenyl)hexafluoropropane dianhydride (6FDA) and some fluorinated diamines own larger CTE, and their Tg are lower 300 °C. Isomeric PIs, which possess geometrically asymmetric and noncoplanar moieties, were found to be endowed with good soluble, thermal and mechanical properties [10,28,29]. Ding's group [30–35] successfully synthesized a series of isomeric PI, and the relationship between structures and properties of isomerized polyimide were summarized [21,22,36]. It was found that

* Corresponding author.
E-mail address: tgl@hust.edu.cn (G. Tu).

http://dx.doi.org/10.1016/j.orgel.2017.09.010
1566-1199/

the isomerized polyimide has higher glass transition temperature (Tg), lower CTE, better solubility, thermal durability and mechanical properties compared with 6FDA based polyimide [22,23].

Herein, we synthesized a series of asymmetric isomeric rigid alicyclic diamines 5-amino-1-(4-aminophenyl)-1,3,3-trimethylindane (5-DAPI), 6-amino-1-(4-aminophenyl)-1,3,3-trimethylindane (6-DAPI), and 5(6)-amino-1-(4-aminophenyl)-1,3,3-trimethylindane (5(6)-DAPI). Experimentally, a series of novel rigid alicyclic functionalized PIs coded as CPI-x (chemical imidization prepared) and TPI-x (thermal imidization prepared), and synthesized through polycondensation of 5-DAPI, 6-DAPI, and 5(6)-DAPI with five different tetracarboxylic dianhydrides. The solubility, thermal durability, the optical, mechanical and surface properties of these flexible substrates were systematic discussed. Ultrathin metal film evaporated on the flexible substrate can be used as an electrode. Nevertheless, the adhesion between film and ultrathin metal was key factor for their application in optoelectronics. It's reported that ultra-thin gold and silver layer was hard to thermal evaporation on the plastic flexible substrate without adhesive layer [37]. In this work, we used MoO_3 (3 nm) as an adhesive layer to improve the adhesion. The ultrathin MoO_3/Au/Ag layer referring to the reported work [38] were deposited on CPI-1 by thermal evaporation was utilized as a transparent bottom electrode, which was applied in QLED and OPV, and exhibited a pretty good devices efficiency.

2. Experimental

2.1. Materials

Dianhydrides, 4,4'-(hexaflouroisopropylidene) diphthalic anhydride (6FDA) 3,3′,4,4′-oxydiphthalic anhydride (ODPA), 3,3′,4,4′-benzophenonetetracarboxylic dianhydride (BTDA), 3,3′,4,4′-biphenyltetracarboxylic dianhydride (BPDA) and pyromellitic dianhydride (PMDA) were purchased from Merck and sublimated before use. Commercially available *N*-methyl-2-pyrrolidinone (NMP), m-cresol, N, *N*-dimethylacetamide (DMAc) were purified by vacuum distillation over P_2O_5 and N, *N*-dimethylformamide (DMF) was purified by vacuum distillation over CaH_2 and then stored over 4 Å molecular sieves prior to use. Other commercially available materials were used without further purification.

2.2. Monomer synthesis of 5-DAPI, 6-DAPI

The synthesis of DAPI, which is the acid catalysed dimerization of α-methylstyrene and subsequent nitration and reduction, has been reported elsewhere [39]. The grey crude isomeric diamine 5(6)-DAPI 10.0 g was sublimated, and had a deep yellow product 9.2 g. The deep yellow product was purified by column chromatography on silica (ethyl acetate/petroleum ether = 7:3) to give 5-DAPI (5.34 g, 20.03 mmol, 58%) as a light yellow solid, and 6-DAPI (3.40 g, 12.78 mmol, 37%) as a light yellow solid. The crude product 5-DAPI and 6-DAPI was then recrystallized from dichloromethane and n-hexane twice to afford white crystals in 48% and 28% yield. The detail measurement of 5-DAPI and 6-DAPI were presented in Supporting Information (Figs. S1, S2, S3 (a)).

2.3. Polymer preparation

A series of polyimide films were prepared by conventional thermal imidization and chemical imidization of 5-DAPI, 6-DAPI, isomeric 5(6)-DAPI with 6FDA, ODPA, BTDA, BPDA and PMDA, respectively. For convenience, the PI films derived from thermal and chemical imidization are coded as CPI-x and TPI-x. The synthesis of the polymers was shown in Fig. 1. (a). The synthesis of TPI-1(5-DAPI/6FDA) is used as an example to illustrate the general thermal imidized synthetic procedure to prepare the polyimide films. 5-DAPI (0.8000 g, 3.004 mmol) was dissolved in 13.1096 g dried NMP in a 50 mL flask, and then 6FDA (1.3342 g, 3.004 mmol) was added to the solution in one portion. The mixture was stirred at room temperature for 24 h to obtain a viscous poly (amic acid) solution. The PAA was subsequently converted into PI by thermal and chemical imidization process. For the thermal imidization, the poly (amic acid) solution was then poured onto a clean glass plate, which was then heated at 80 °C for 2 h for the slow release of the solvent, and sequential heating at 100 °C for 1 h, 150 °C for 1 h, 200 °C for 1 h, 250 °C for 1 h, and 280 °C for 1 h. TPI-1 was released from the glass surface after being soaked in deionized water. Meanwhile, the chemical imidization was carried out via the addition of 2.5 mL of an acetic anhydride/triethylamine (1:1, v/v) mixture into the PAA solution with stirring at room temperature. Then, the mixture was heated to 60 °C for 24 h to yield a homogeneous PI solution. The solution was then poured onto a clean glass plate, and removed the solvent with the same procedure with thermal imidization.

2.4. Transparent flexible electrode fabrication

The glass (size of 2.5 cm × 2.5 cm) and films (2.5 cm × 2.5 cm) were ultrasonic cleaned with deionized water twice (30 min). After the completion of ultrasonic cleaning with nitrogen, and then move into the oven at 150 °C for 30 min. After cooling at room temperature, using the high temperature tape to make the film cling to the glass tightly. Then, the MoO_3, Au, and Ag were fabricated by thermal evaporation technology under pressure below 1.5×10^{-4} Pa in the surface of PI films. The deposition current was about 40 A, 90 A, and 30 A, the thickness was controlled by a quartz oscillating thickness monitor [38]. The layer thicknesses were 3, 2, and 4 nm for MoO_3, Au, and Ag, respectively.

2.5. Device fabrication

The QLED fabrication were referred to the literature, which possessing the structure of PI/(MoO_3/Au/Ag)/ZnO/QDs/4,4′-*N*,*N*′-dicarbazole-biphenyl (CBP)/MoO_3/Al [40]. The ZnO precursor solution were spin coated on the polyimide/electrode substrate treated with O_2 plasma and baked at 220 °C for 30 min in a glove box filled with nitrogen. Then, CdSe/CdS/ZnS QDs (from Poly Opto Electronics Co., Ltd.) in octane (5 mg/mL) were spin-coated on the ZnO film and baked at 100 °C for 10 min. After completion of the solution process, the substrate was transferred to a vacuum chamber for the overlying organic film and MoO_3 (10 nm) and Al (100 nm) electrode deposition with the base pressure of 4×10^{-4} Pa. The area of the device was 9.0 mm^2. Meanwhile, the OPV device was fabricated with the architecture of PI/cathode/ZnO/PTB7: $PC_{71}BM$/MoO_3/Ag. The active layer PTB7:$PC_{71}BM$ (1:1.5 in wt %) was dissolved in chlorobenzene at the overall concentration of 25 mg/mL with 3 vol % DIO. Next, MoO_3 (10 nm) and the Ag electrode (100 nm) was thermally deposited on top of the active layer at 2×10^{-4} Pa.

3. Results and discussion

The spatial configuration of the monomer was measured by the single crystal diffraction and a larger dihedral angle of 5-DAPI (85.7°) than that of 6-DAPI (78.2°) was observed in Fig. 1(b)-(c). As a consequence, the steric effect and asymmetric degree of 6-DAPI is stronger than that of 5-DAPI. The IR (cm^{-1}, film) were measured to testify the polymerization of monomer: 1781, 1728(imide carbonyl *asym*. and *sym*. stretching), 1385 (C—N

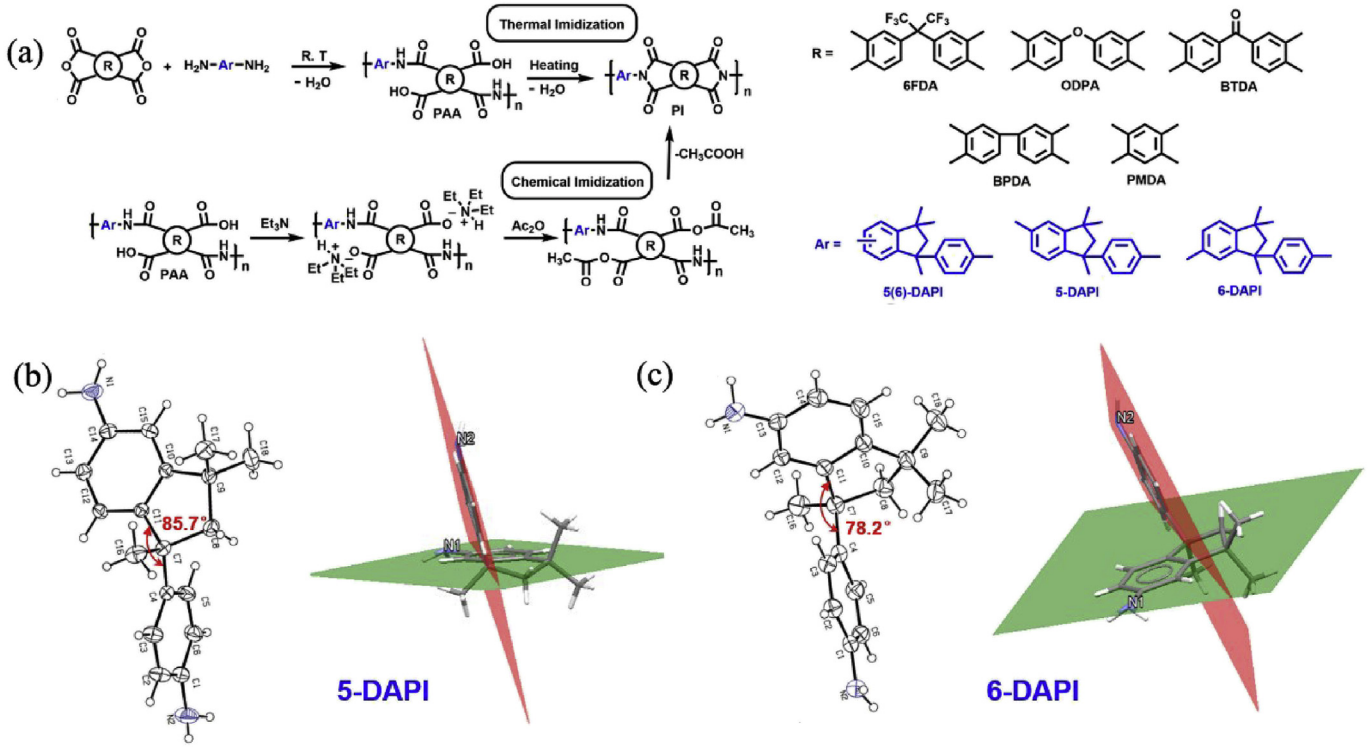

Fig. 1. (a) The synthesis of the polyimide films. (b) Molecular structure and dihedral angle of 5-amino-1-(4-aminophenyl)-1, 3, 3-trimethylindane. (c) Molecular structure and dihedral angle of 6-amino-1-(4-aminophenyl)-1, 3, 3-trimethylindane.

stretching), 1121, 727 (imide ring deformation), IR (cm^{-1}, film): 1780, 1726 (imide carbonyl *asym*. and *sym*. stretching), 1385 (C—N stretching), 1119, 727 (imide ring deformation). The IR spectra of CPI-x and TPI-x was shown in Supporting Information Fig. S3 (b)-(f). The optical, thermal, mechanical, surface and dielectric properties of the polyimide films were measured to testify how the asymmetric rigid alicyclic influence their applicability for transparent flexible substrate, respectively. Due to the 5-DAPI possessing bigger dihedral angle than 6-DAPI, which reduced intermolecular dipole-dipole interaction based on the much bent/nonplanar steric structure of 5-DAPI. Such a structure also decreased the chain packing and increased the average distance of chain, improved solubility of 5-DAPI based films better than 6-DAPI. The solubility of films depicted in Supporting Information, and all summarized in Table S1 and Fig. S4.

3.1. Optical properties of PIs

The transmittance at 450 nm (T_{450}) and UV cutoff wavelength (λ_0) were summarized into Table 1. In addition, the UV—Vis spectra of all CPI-x films and TPI-x films were shown in Fig. S5 (a-b). From the curve displayed in Fig. 2(a), by comparison, polyimides from 5-DAPI possessed best optical properties among 6-DAPI and 5(6)-DAPI PIs. The optical transparency differences between 5-DAPI, 6-DAPI and 5(6)-DAPI series are explainable by the decreased CTC formation. The presence of bigger dihedral angle of 5-DAPI can decrease the steric hindrance of backbone, break the conjugation of the polymer chain, increase the free volume and thus segments the charge transfer pathway [41]. So that 5-DAPI series holding better transmittance than its analogous PIs. CPI-x enjoys higher optical transparency than its corresponding TPI-x. For instance, CPI-1 and CPI-3 show T_{450} over 80% and λ_0 below 370 nm. Whereas, T_{450} values of the homologous series TPI-1 and TPI-2 are lower than 80% and λ_0 values above 370 nm of the polymers. Due to the processing of thermal imidization, TPI-x was easy to occur crosslink between intermolecular chains, and increasing the packing degree, reducing the optical properties of TPI-x [42]. Moreover, the CPI-x gets isotropic state of aggregation, and lower degree of crystallinity that contribute to its better transmittance. The CPI-1 film based on 5-DAPI and 6FDA showed the best transmittance of 82.9% at

Table 1
The thermal resistant, mechanical, optical and surface properties of PI films.

Polymer	Dianhydride	Dianmine	Thermal properties				Mechanical properties[a]			Optical properties		Surface properties	
			T_g(°C) DMA	T_{d5} (°C)	T_{d10} (°C)	Char Yield(%)[b]	T_s (MPa)	E_b (%)	T_m (GPa)	T_{450}[c] (%)	λ_0[d] (nm	Contact angle[e] (°)	RMS (nm)
CPI-1	6FDA	5DAPI	333.1	494	510	57.9	91.6	8.8	2.1	82.9	361	99.1	0.78
CPI-2	6FDA	6DAPI	345.2	504	522	56.1	53.8	4.8	1.5	82.6	366	93.6	0.82
CPI-3	6FDA	Isomer	335.9	496	512	57.1	56.2	4.1	2.1	78.5	365	96.8	1.18

[a] T_s, tensile strength; E_b, elongation at break; T_m, tensile modulus.
[b] Residual weight percentage at 800 °C in N_2.
[c] Transmittance at 450 nm.
[d] UV—vis cutoff wavelength.
[e] Equilibrium contact angle was measured at ambient temperature and double distilled water as solvent for a time period of 120 s depending on the stability of the drop, and the data were the average value of 10 experiments.

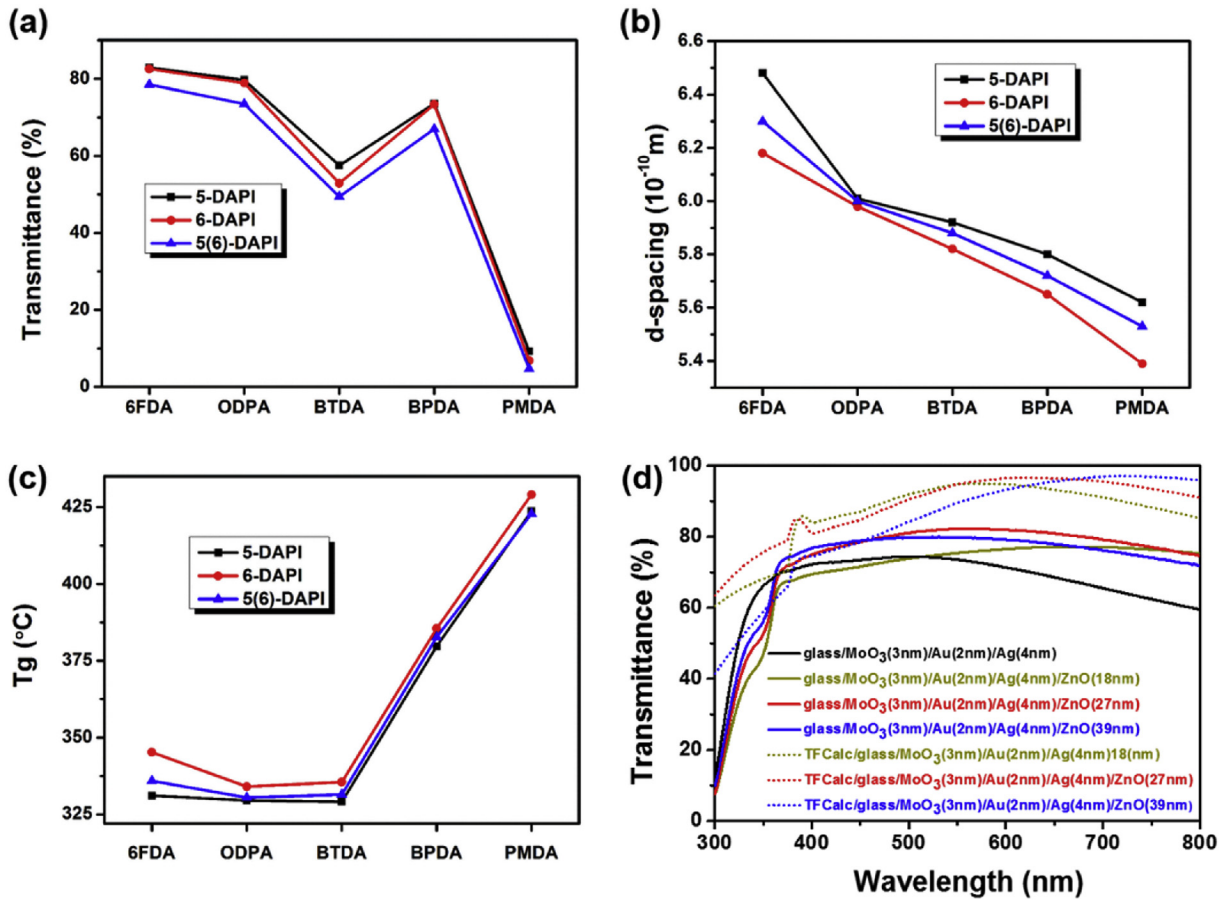

Fig. 2. (a) Transmittance of PI films derived from isomeric diamine and various anhydrides. (b) d-spacing of PI films derived from isomeric diamine and various anhydrides. (c) Tg of PI films derived from isomeric diamine and various anhydrides. (d) Transmittance of the flexible electrode containing different thickness of ZnO layer.

450 nm, which meets the applicable properties criterion for advanced optoelectronics. 6FDA series PIs have strong electron-withdrawing trifluoromethyl group in diamine moieties are presumably effective in decreasing the inter-chain CTC [43,44], and consequently results in the reduced coloration and the improved transparence of the films. The biggest d-spacing of PIs based on 5-DAPI shown in Fig. 2(b) was another proof of the good transmittance.

3.2. Thermal properties of PIs

The thermal decomposition and stability of the TPI-x and CPI-x were evaluated by TGA and DMA. The results were shown in Table 1. All data were obtained from the PIs films. The Tg values of TPI-x were in the range of 321–370 °C, while the Tg of CPI-x were in the range of 329–429 °C. Interestingly, from Figs. 2(c) and 3 (a)-(b), we found that all 6-DAPI derived polymers had higher Tg values than corresponding 5-DAPI polymers, and the Tg of films originated from 5(6)-DAPI between the PIs behind. And the dates also indicated that the Tg of CPI-x was bigger than TPI-x. Fig. 3 (a)-(b) and Fig. S6 (a)-(c), displaying the glass transition temperature of the films. For instance, the polymer 6-DAPI/6FDA showed a higher Tg at 345 °C than the polymer 5-DAPI/6FDA at 334 °C. This might be attributed to steric hindrance of DAPI structure. PIs derive from the same dianhydrides based on 6-DAPI owned highest Tg values among these analogous PIs [45]. Meanwhile Tg of CPI-x (CPI-4, ODPA/5-DAPI, 329.5 °C) was bigger than homologous TPI-x (TPI-3, ODPA/5-DAPI, 321.9 °C), which was attributed to different imidization processes. In the case of chemical imidization, water is not generated directly, and polymerization reacted at a moderate temperature and the presence of triethylamine makes the solution alkaline, meanwhile hydrolysis of the PAA is inhibited [46]. Polymer with the same structure, the bigger molecular weight, the higher Tg, and CPI-x has bigger molecular weight lead to the Tg was significantly higher than the corresponding TPI-x.

A typical set of TGA curves for CPI-(1–3) were depicted in Fig. 3 (c)-(d) and Fig. S6 (d)-(f). No weight loss was detected until the temperature was scanned up to 480 °C. The T_{d10} of CPI-x in N_2 stays in the range of 510–522 °C. The results indicated that these PI films owned excellent thermal stability.

3.3. Mechanical and surface properties of the PIs

Mechanical properties of the PIs were summarized in Table 1. The depicted stress-strain curves were shown in Supporting Information Fig. S7. CPI-x series show tensile strengths at break of 45.7–103.0 MPa, elongation at break of 2.7–11.2%, and tensile modulus of 1.5–2.8 GPa. By contrast, TPI-x series showed tensile strengths of 16.0–80.7 MPa, elongation at break of 0.8–8.2%, and tensile modulus of 1.7–2.1 GPa. It was found that CPI-x displayed excellent mechanical properties than TPI-x. The larger tensile strengths, elongation at break and tensile modulus of CPI-x could be owed to their preparation process. PIs prepared from chemical imidization have a bigger molecular weight and longer chain, it's reported that PIs with the same structure, the longer molecular chain, the greater accumulation of the main chain it was [47]. It was

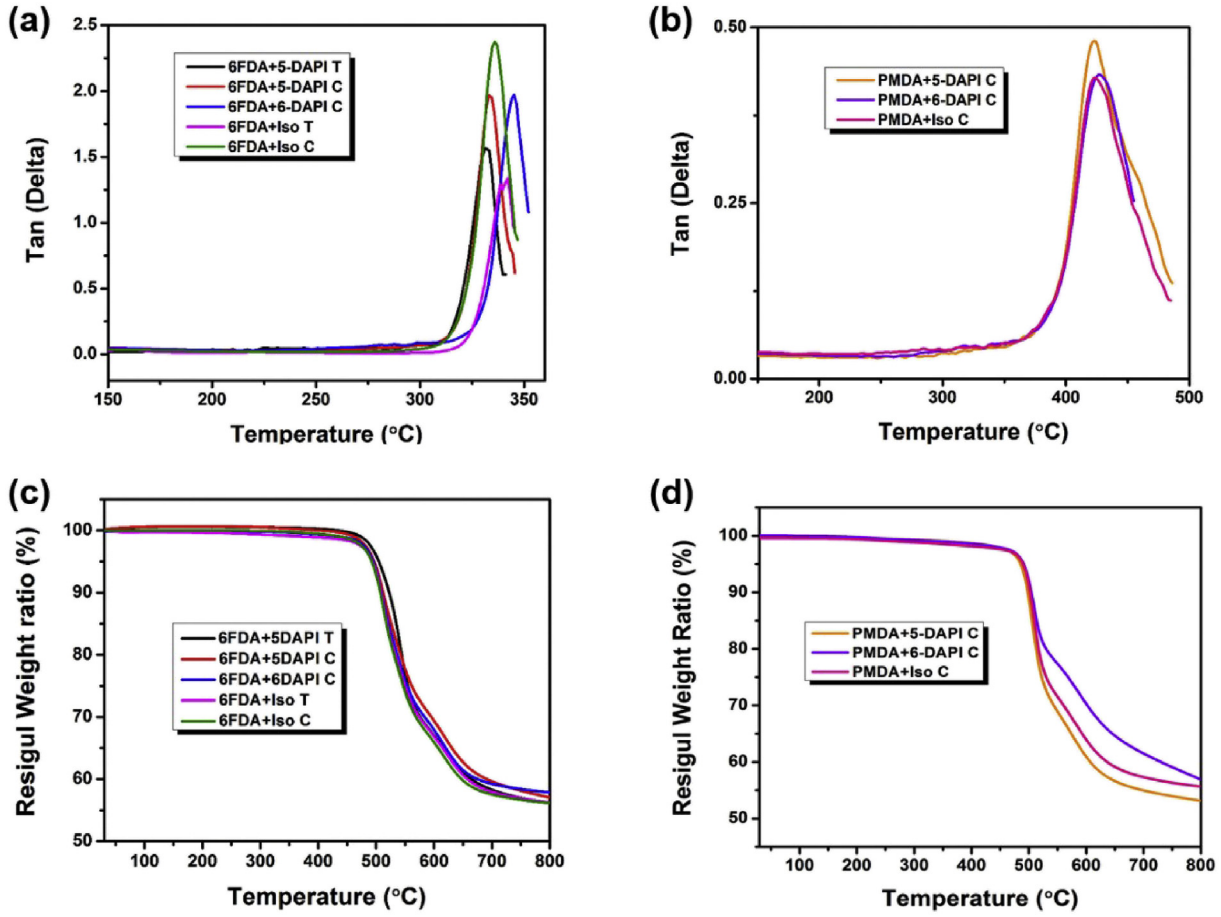

Fig. 3. (a) DMA curve of PIs based on 6FDA and diamines. (b) DMA curve of PIs based on PMDA and diamines. (c) TGA curve of PIs based on 6FDA and diamines. (d) TGA curve of PIs based on PMDA and diamines.

made the macromolecular hard to slide, and showing stronger rigidity, holding greater elastic modulus and tensile strengths [28]. Both series followed the tendency toward same dianhydride variation on the decreasing order for 5-DAPI > 5(6)-DAPI > 6-DAPI in terms of tensile strengths elongation at break, and tensile modulus.

The average values of these AFM surface relief parameters are obtained from three different 2 × 2 μm^2 images as seen in Fig. S8, for each sample. And the root mean square (RMS) roughness displayed in Table S2. Generally, RMS strongly interrelating with the degrees of order or disorder in the grain structure distribution and associated with the shape-size complexity [48]. So that PI-x based on 5-DAPI with more regular structure having the lowest RMS values. For instance, RMS value of CPI-1 (5-DAPI/6FDA) is 0.78 nm, while CPI-2 (6-DAPI/6FDA) is 0.82 nm. From the date shown in Table S2, all PIs possessed small RMS, it's a critical factor of PI films used as flexible substrate. The results indicated that CPI-1 can not only be used to prepare ITO electrode, but also as flexible substrate for ultra-thin metal electrodes. The contact angles against water, surface energy and moisture uptakes of PI films were detailed in supporting information Fig. S9.

Integrated the factors above, we chose CPI-1 as transparent and thermal resistant substrate.

3.4. Electrode properties

The transmittance, electron conductivity, adhesion and bending resistant performance were shown in Fig. 2 (d), Fig. S11 and summarized in Table S3 and Table S4. As it was depicted in Fig. 2 (d), the biggest transmittance of PI substrate was 69.3%. After a ZnO layer was spin-coated on the PI/MoO_3/electrode substrate and annealed at 220 °C for 30 min, the transmittance can be increased to the 80.8%. It can be explained that ZnO layer decreased the surface reflection of the silver layer and increased the transmittance of the metal electrode. Moreover, the TFCalc (Software for the Design and Manufacture of Optical Thin Film) was used to calculate the transmittance of electrode with ZnO layer, as it was shown in Fig. 2(d), the TFCalc calculate result shows that the 27 nm ZnO is the optimal thickness in consideration of optical transparency, which in line with the experimental result. The higher transmittance would benefit for the efficiency of QLED and OPV device. We have measured the morphology of the bottom layer to testify whether substrate affect the upper active layer. From Fig. 4, after coating various thickness ZnO layer on MoO3/Au/Ag electrode on glass and PI substrate, the RMS presented no obvious difference between glass Fig. 4 (a)-(c) and PI substrate Fig. 4 (d)-(f), thus, the bottom layer would have negligible effect on the upper active layer morphology. The square resistance (R_{sq}) of the flexible electrode (45.2 Ω/sq) was measured by a four-probe resistivity instrument, it was not much different from that on the glass substrate (35.5Ω/sq). In order to investigate the adhesion of the transparent conductive electrode with the PI film, we used tape to adhere to the electrode, and then tear off the tape to measure the R_{sq} of the electrode. Repeated this step four times at the same location for each measurement of the R_{sq}, and shown in Table S3. It can be seen that the

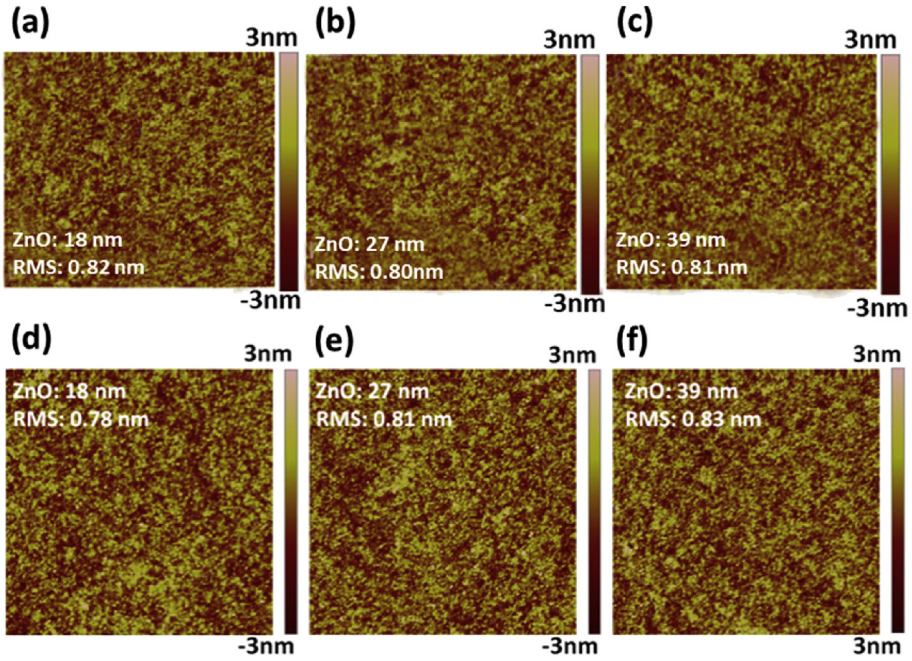

Fig. 4. (a) The AFM images of glass electrode with 18 nm ZnO layer. (b) The AFM images of glass electrode with 27 nm ZnO layer. (c) The AFM images of glass electrode with 39 nm ZnO layer. (d) The AFM images of flexible electrode with 18 nm ZnO layer. (e) The AFM images of flexible electrode with 27 nm ZnO layer. (f) The AFM images of flexible electrode with 39 nm ZnO layer.

R_{sq} is not changed obviously after four times test, indicating that the electrode possessed good adhesion with the PI substrate. To further test the mechanical properties of the flexible electrode, the bending measurement was taken as shown in insets of Fig. S11 (b), the R_{sq} of the electrode was tested after several times of bending and the experimental results was shown in Fig. S11 (b). We found that the flexible transparent electrode owned good mechanical properties after 100 times of bending, and the R_{sq} was not changed obviously. In summary, the ultrathin metal multilayer electrode based on PI film has good photoelectric properties, good adhesion and excellent mechanical performances, which indicating that PI/(MoO_3/Au/Ag) could be a promising transparent flexible electrode for optoelectronics devices.

3.5. QLED device properties

As discussion above, the polyimide based 5-DAPI with good optical, mechanical, surface and dielectric properties was chosen as the flexible substrate. The QLED were fabricated with the structure of PI/(MoO_3/Au/Ag)/ZnO/QDs/CBP/MoO_3/Al, in which the CdSe/CdS/ZnS quantum dot (QD) was used as the emitting material, shown in Fig. 5 (a). Fig. 5 (b) schematically shows the energy level diagram of the devices and demonstrates the holes and electrons can be easily injected and recombine in the emitting layer through the ZnO layer and CBP layer, respectively. The luminance, current density, external quantum efficiency (EQE), was shown in Fig. 5(c) and (d), respectively. The QLED based on glass substrate and flexible substrate show luminance of 5160 cd/m^2 and 5230 cd/m^2, and highest EQE of 5.5% and 5.2%, respectively. The QLED performance based on PI substrate is lower than the glass ones. That may result from the lower optical transparency, higher Rsq, not good flexible device fabrication process. These results indicated that the PI substrates could be used as a promising flexible and transparent substrates for QLED.

3.6. OPV device properties

To testify the universality of the 5-DAPI based polyimide substrate, the inverted solar cell devices with architecture of PI/cathode/ZnO/PTB7:$PC_{71}BM$/MoO_3/Ag were also employed. The structure and the current density versus voltage (J-V) curves were shown in Fig. 5(e)-(f) and summarized in Table S5, the open-circuit voltage of 0.71 V and power efficiency of 4.36% were obtained. However, the differences in optical transmission between PI and glass substrate electrode, causing the lower fill factor and current density of the PI devices with contrastive glass devices. The lower fill factor for the PI based solar cell may come from lots of factor, the Rsq, electron conductivity, morphology of the active layer. As we mentioned above, the bottom layer would have negligible effect on the upper active layer morphology. And the four probe method was unitized to measure the Rsq of the MoO_3/Au/Ag electrode on the glass and PI substrate, and the Rsq of the glass and PI substrate electrode are 35.5 and 45.2 Ω/sq, respectively. The difference of Rsq actually affect the short circuit current and fill factor. Therefore, PI based OPV devices can be a promising way to get flexible and high power efficiency OPVs by optimizing the electrode.

4. Conclusions

In conclusion, we have successfully synthesized a series of isomeric PI films. All of the films shown outstanding thermal resistant attributing to disturbed chain stacking by a twist/nonplanar steric structure of the DAPI based diamine fragments. Systematic study revealed that PI based on 5-DAPI displayed much better optical, mechanical, and surface properties than 6-DAPI. Therefore, CPI-1 based 5-DAPI was chosen as the flexible substrate, and MoO_3/Au/Ag layer were fabricated by thermal evaporation on the surface of CPI-1. The preferable transmittance, R_{sq}, and bending resistant properties of the PI/(MoO_3/Au/Ag) shown that it can be utilized as a flexible transparent electrode for optoelectronics. As a result, the QLED obtained a high luminance of 5230 (cd/m^2) and

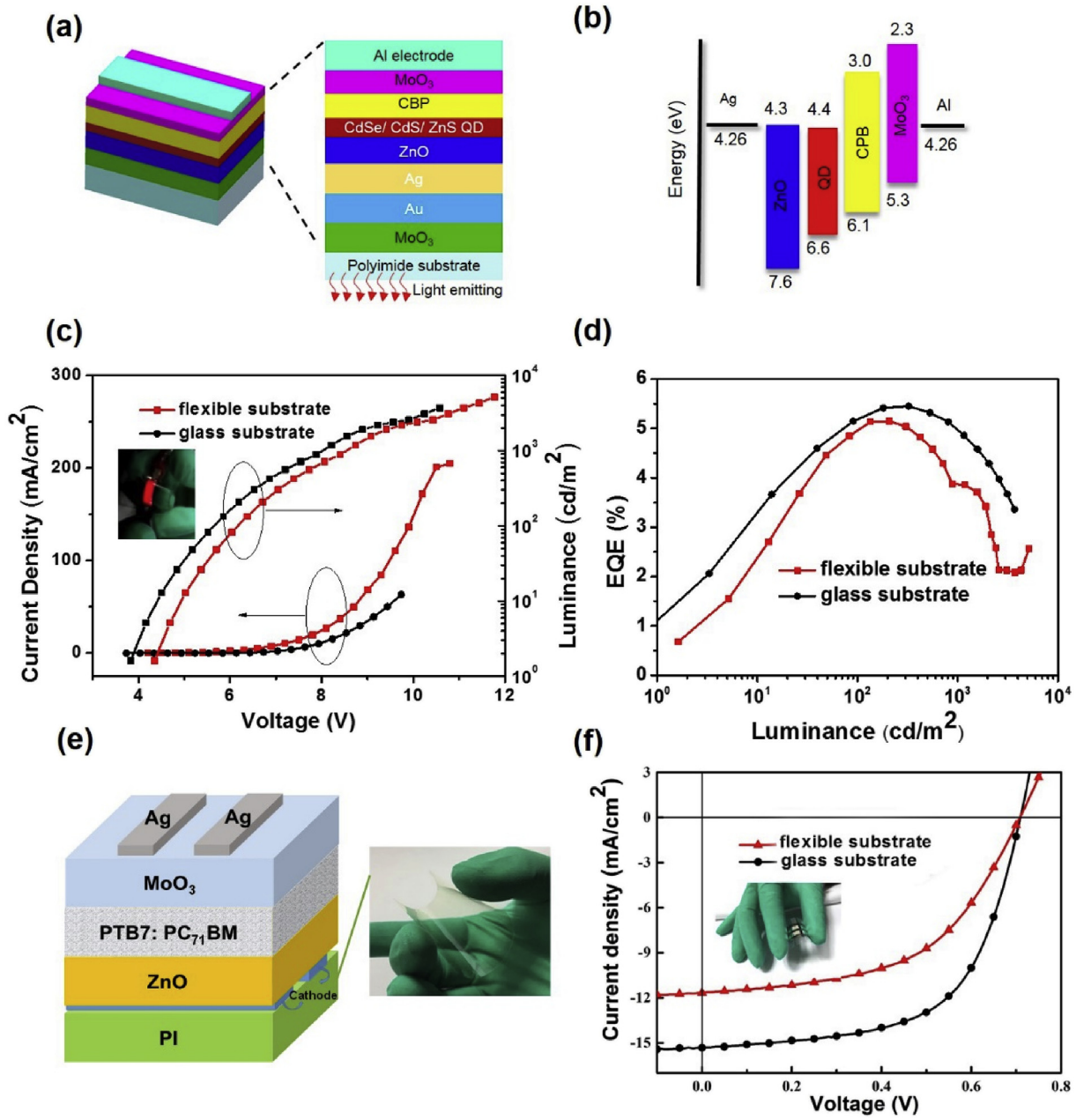

Fig. 5. (a) Schematic of the QLED configuration; (b) Energy level diagram of the fabricated QLEDs; (c) EL spectra of QLEDs; (d) EQE versus luminance characteristics. (e) Structure of organic photovoltaic devices. (f) The current density versus voltage (J–V) curves of OPVs based on glass or PI substrate.

EQE of 5.2%, meanwhile, a device performance of 4.36% was achieved in OPV devices. These results suggest that the DAPI-based PIs can be promising candidates for novel optical components as thermal durability plastic substrates in flexible OLED display, wearable device, and others.

Acknowledgements

This work was financially supported by the National Natural Science Foundation of China (21574049), and the National High Technology Research and Development Program of China (863 Program, No. 2015AA033404) for financial support. We also thanks to the HUST Analytical and Testing Center for allowing us to use its facilities.

Appendix A. Supplementary data

Supplementary data related to this article can be found at http://dx.doi.org/10.1016/j.orgel.2017.09.010.

References

[1] D. Ma, M. Lv, M. Lei, J. Zhu, H. Wang, X. Chen, Self-organization of amine-based cathode interfacial materials in inverted polymer solar cells, ACS Nano 8 (2014) 1601–1608.
[2] J.A. Spechler, T.-W. Koh, J.T. Herb, B.P. Rand, C.B. Arnold, A transparent, smooth, thermally robust, conductive polyimide for flexible electronics, Adv. Funct. Mater. 25 (2015) 7428–7434.
[3] Z. Xu, M. Li, M. Xu, J. Zou, H. Tao, L. Wang, J. Peng, Light extraction of flexible OLEDs based on transparent polyimide substrates with 3-D photonic structure, Org. Electron. 44 (2017) 225–231.
[4] B.J. Richardson, L. Zhu, Q. Yu, Design and development of plasmonic

nanostructured electrodes for ITO-free organic photovoltaic cells on rigid and highly flexible substrates, Nanotechnology 28 (2017) 165401.
[5] J. Park, B.G. Hyun, B.W. An, H.G. Im, Y.G. Park, J. Jang, J.U. Park, B.S. Bae, Flexible transparent conductive films with high performance and reliability using hybrid structures of continuous metal nanofiber networks for flexible opto-electronics, ACS Appl. Mater Interfaces 9 (2017) 20299–20305.
[6] Y. Park, F. Nehm, L. Muller-Meskamp, K. Vandewal, K. Leo, Optical display film as flexible and light trapping substrate for organic photovoltaics, Opt. Express 24 (2016). A974–980.
[7] Y. Park, J. Berger, Z. Tang, L. Müller-Meskamp, A.F. Lasagni, K. Vandewal, K. Leo, Flexible, light trapping substrates for organic photovoltaics, Appl. Phys. Lett. 109 (2016), 093301(1-5).
[8] E. Jung, C. Kim, M. Kim, H. Chae, J.H. Cho, S.M. Cho, Roll-to-roll preparation of silver-nanowire transparent electrode and its application to large-area organic light-emitting diodes, Org. Electron. 41 (2017) 190–197.
[9] Y.-Y. Yu, T.-J. Huang, W.-Y. Lee, Y.-C. Chen, C.-C. Kuo, Highly transparent polyimide/nanocrystalline-zirconium dioxide hybrid materials for organic thin film transistor applications, Org. Electron. 48 (2017) 19–28.
[10] H.P. Wu, Q. Yang, Q.H. Meng, A. Ahmad, M. Zhang, L.Y. Zhu, Y.G. Liu, Z.X. Wei, A polyimide derivative containing different carbonyl groups for flexible lithium ion batteries, J. Mater. Chem. A 4 (2016) 2115–2121.
[11] K. Ding, H. Chen, L. Fan, B. Wang, Z. Huang, S. Zhuang, B. Hu, L. Wang, Polyethylenimine insulativity-dominant charge-injection balance for highly efficient inverted quantum dot light-emitting diodes, ACS Appl. Mater. Interfaces 9 (2017) 20231–20238.
[12] J. Shen, F. Li, Z. Cao, D. Barat, G. Tu, Light scattering in nanoparticle doped transparent polyimide substrates, ACS Appl. Mater Interfaces 9 (2017) 14990–14997.
[13] K.H.M. Hasegawa, Photophysics, photochemistry, and optical properties of polyimides, Prog. Polym. Sci. 26 (2001) 259–335.
[14] D.H. Wang, J.J. Wie, K.M. Lee, T.J. White, L.-S. Tan, Impact of backbone rigidity on the photomechanical response of glassy, azobenzene-functionalized polyimides, Macromolecules 47 (2014) 659–667.
[15] H.S. Kim, Y.H. Kim, S.K. Ahn, S.K. Kwon, Synthesis and characterization of highly soluble and oxygen permeable new polyimides bearing a noncoplanar twisted biphenyl unit containing tert-butylphenyl or trimethylsilyl phenyl groups, Macromolecules 36 (2003) 2327–2332.
[16] D.-J. Liaw, K.-L. Wang, Y.-C. Huang, K.-R. Lee, J.-Y. Lai, C.-S. Ha, Advanced polyimide materials: syntheses, physical properties and applications, Prog. Polym. Sci. 37 (2012) 907–974.
[17] H.-C. Yu, J.-W. Jung, J.-Y. Choi, C.-M. Chung, Kinetic study of low-temperature imidization of poly(amic acid)s and preparation of colorless, transparent polyimide films, J. Polym. Sci. Part A Polym. Chem. 54 (2016) 1593–1602.
[18] M. Jia, Y. Li, C. He, X. Huang, Soluble perfluorocyclobutyl aryl ether-based polyimide for high-performance dielectric material, ACS Appl. Mater. Interfaces 8 (2016) 26352–26358.
[19] Y. Ding, H. Hou, Y. Zhao, Z. Zhu, H. Fong, Electrospun polyimide nanofibers and their applications, Prog. Polym. Sci. 61 (2016) 67–103.
[20] W.J. Bae, M.K. Kovalev, F. Kalinina, M. Kim, C. Cho, Towards colorless polyimide/silica hybrids for flexible substrates, Polymer 105 (2016) 124–132.
[21] H. Borjigin, Q. Liu, W. Zhang, K. Gaines, J.S. Riffle, D.R. Paul, B.D. Freeman, J.E. McGrath, Synthesis and characterization of thermally rearranged (TR) polybenzoxazoles: influence of isomeric structure on gas transport properties, Polymer 75 (2015) 199–210.
[22] Y. Zhang, J. Shen, Q. Zhang, Z. Xu, K.W.K. Yeung, C. Yi, Review on F, Si and P-Containing polyimides with special properties, Sci. Adv. Mater. 6 (2014) 44–55.
[23] P. Suvannasara, S. Tateyama, A. Miyasato, K. Matsumura, T. Shimoda, T. Ito, Y. Yamagata, T. Fujita, N. Takaya, T. Kaneko, Biobased polyimides from 4-aminocinnamic acid photodimer, Macromolecules 47 (2014) 1586–1593.
[24] Y. Liu, D. Chao, H. Yao, New triphenylamine-based poly(amine-imide)s with carbazole-substituents for electrochromic applications, Org. Electron. 15 (2014) 1422–1431.
[25] K.H. Ok, J. Kim, S.R. Park, Y. Kim, C.J. Lee, S.J. Hong, M.G. Kwak, N. Kim, C.J. Han, J.W. Kim, Ultra-thin and smooth transparent electrode for flexible and leakage-free organic light-emitting diodes, Sci. Rep. 5 (2015), 9464(1-5).
[26] C.-L. Tsai, T.-M. Lee, G.-S. Liou, Novel solution-processable functional polyimide/ZrO2hybrids with tunable digital memory behaviors, Polym. Chem. 7 (2016) 4873–4880.
[27] J.-M. Won, H.J. Suk, D. Wee, Y.H. Kim, J.-W. Ka, J. Kim, T. Ahn, M.H. Yi, K.-S. Jang, Photo-patternable polyimide gate insulator with fluorine groups for improving performance of 2,7-didecyl[1]benzothieno[3,2-b][1]benzothiopene (C10-BTBT) thin-film transistors, Org. Electron. 14 (2013) 1777–1786.
[28] M.X. Ding, Isomeric polyimides, Prog. Polym. Sci. 32 (2007) 623–668.
[29] N. Mushtaq, G. Chen, L.R. Sidra, Y. Liu, X. Fang, Synthesis and crosslinking study of isomeric poly(thioether ether imide)s containing pendant nitrile and terminal phthalonitrile groups, Polym. Chem. 7 (2016) 7427–7435.
[30] M. Zhang, Z. Wang, L. Gao, M. Ding, Polyimides from isomeric diphenylthioether dianhydrides, J. Polym. Sci. Part A Polym. Chem. 44 (2006) 959–967.
[31] X.Z. Fang, Q.X. Li, Z. Wang, Z.H. Yang, L.X. Gao, M.X. Ding, Synthesis and properties of novel polyimides derived from 2,2',3,3'-benzophenonetetracarboxylic dianhydride, J. Polym. Sci. Part A Polym. Chem. 42 (2004) 2130–2144.
[32] Q.X. Li, X.Z. Fang, Z. Wang, L.X. Gao, M.X. Ding, Polyimides from isomeric oxydiphthalic anhydrides, J. Polym. Sci. Part A Polym. Chem. 41 (2003) 3249–3260.
[33] Y.J. Tong, W.X. Huang, J. Luo, M.X. Ding, Synthesis and properties of aromatic polyimides derived from 2,2',3,3'-biphenyltetracarboxylic dianhydride, J. Polym. Sci. Part A Polym. Chem. 37 (1999) 1425–1433.
[34] Y.S. Li, M.X. Ding, J.P. Xu, Gas permeability in polyimides from oxydianiline and isomeric thiaphthalic dianhydride or 1,4-bis(dicarboxyphenoxy) benzene dianhydride, Polymer 37 (1996) 3451–3453.
[35] M.X. Ding, H.Y. Li, Z.H. Yang, Y.S. Li, J. Zhang, X.Q. Wang, Comparative study on polyimides from 3,3'- and 4,4'-linked diphthalic anhydride, J. Appl. Polym. Sci. 59 (1996) 923–930.
[36] H.-C. Yu, S.V. Kumar, J.H. Lee, S.Y. Oh, C.-M. Chung, Preparation of robust, flexible, transparent films from partially aliphatic copolyimides, Macromol. Res. 23 (2015) 566–573.
[37] J. Hwang, A. Wan, A. Kahn, Energetics of metal–organic interfaces: new experiments and assessment of the field, Mater. Sci. Eng. R. 64 (2009) 1–31.
[38] S. Lenk, T. Schwab, S. Schubert, L. Müller-Meskamp, K. Leo, M.C. Gather, S. Reineke, White organic light-emitting diodes with 4 nm metal electrode, Appl. Phys. Lett. 107 (2015), 163302(1-4).
[39] I.V. Farr, T.E. Glass, Q. Ji, J.E. McGrath, Synthesis and characterization of diaminophenylindane based polyimides via ester-acid solution imidization, High. Perform. Polym. 9 (1997) 345–352.
[40] Y. Fang, K. Ding, Z. Wu, H. Chen, W. Li, S. Zhao, Y. Zhang, L. Wang, J. Zhou, B. Hu, Architectural engineering of nanowire network fine pattern for 30 mum wide flexible quantum dot light-emitting diode application, ACS Nano 10 (2016) 10023–10030.
[41] F. Li, W.J. Wan, J.C. Lai, F. Liu, H.X. Qi, X.S. Li, X.Z. You, Investigations on the polyimides derived from unfunctionalized symmetric cyclopentyl-containing alicyclic cardo-type dianhydride, J. Appl. Polym. Sci. 132 (2015), 42670(1-10).
[42] W. Chen, W. Chen, B. Zhang, S. Yang, C.-Y. Liu, Thermal imidization process of polyimide film: interplay between solvent evaporation and imidization, Polymer 109 (2017) 205–215.
[43] C.-L. Chung, W.-F. Lee, C.-H. Lin, S.-H. Hsiao, Highly soluble fluorinated polyimides based on an asymmetric bis(ether amine): 1,7-bis(4-amino-2-trifluoromethylphenoxy)naphthalene, J. Polym. Sci. Part A Polym. Chem. 47 (2009) 1756–1770.
[44] X. Wang, F. Liu, J. Lai, Z. Fu, X. You, Comparative investigations on the effects of pendent trifluoromethyl group to the properties of the polyimides containing diphenyl-substituted cyclopentyl Cardo-structure, J. Fluor. Chem. 164 (2014) 27–37.
[45] Y. Zhuang, J.G. Seong, Y.S. Do, H.J. Jo, M.J. Lee, G. Wang, M.D. Guiver, Y.M. Lee, Effect of isomerism on molecular packing and gas transport properties of poly(benzoxazole-co-imide)s, Macromolecules 47 (2014) 7947–7957.
[46] Z. Hu, M. Wang, S. Li, X. Liu, J. Wu, Ortho alkyl substituents effect on solubility and thermal properties of fluorenyl cardo polyimides, Polymer 46 (2005) 5278–5283.
[47] B. Comesaña-Gándara, M. Calle, H.J. Jo, A. Hernández, J.G. de la Campa, J. de Abajo, A.E. Lozano, Y.M. Lee, Thermally rearranged polybenzoxazoles membranes with biphenyl moieties: monomer isomeric effect, J. Membr. Sci. 450 (2014) 369–379.
[48] A.I. Barzic, I. Stoica, N. Fifere, C.D. Vlad, C. Hulubei, Morphological effects on transparency and absorption edges of some semi-alicyclic polyimides, J. Polym. Res. 20 (2013), 130 (1-8).